Supporting Information

Chemically Specific Dynamic Bond Percolation Model for Ion Transport in Polymer Electrolytes

Michael A. Webb, Brett M. Savoie, Zhen-Gang Wang, and Thomas F. Miller III*

Division of Chemistry and Chemical Engineering, California Institute of Technology, Pasadena, California 91125, USA

E-mail: tfm@caltech.edu

Contents

*To whom correspondence should be addressed

1 Force Field Parameters for Molecular Dynamics Simulations

In this section, the parameters used to perform the MD simulations are provided. As discussed in the main text, the generalized CHARMM bonding parameters are used,[1] and the TraPPE-UA force field is used for all other inter- and intramolecular interactions between polymer atoms.[2,3] Parameters for the lithium cation are obtained from a previous simulation study.[4] Figure S1 provides reference labels for the different atom types for assigning the appropriate force field parameters.

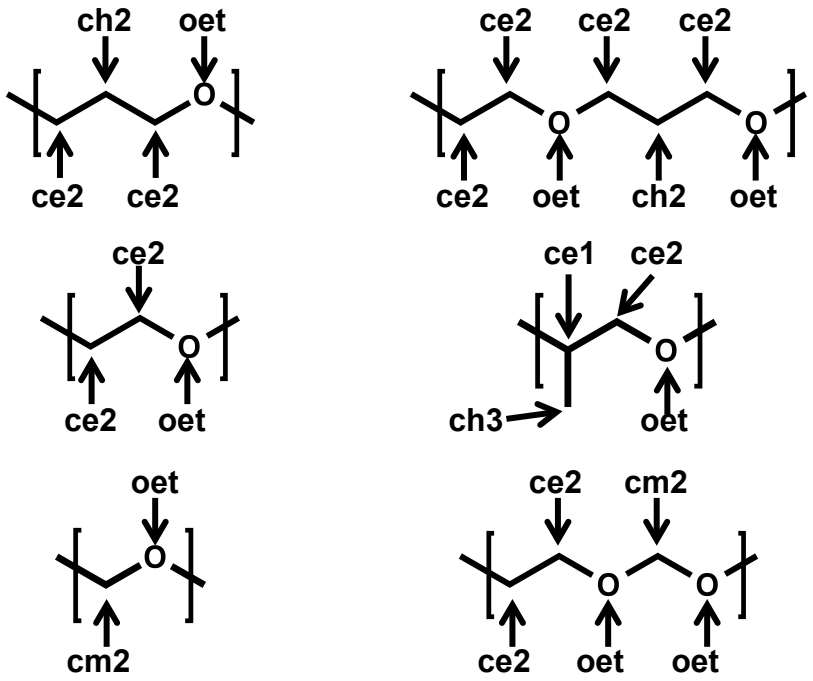

Figure S1: Reference labels for atom types in force field parameters.

1.1 Non-bonded Interaction Parameters

Non-bonded interactions are computed for all intermolecular interactions and for intramolecular interactions between atoms separated by four or more bonds and consist of pairwise

additive Lennard-Jones and Coulombic potentials

$$u_{\mathrm{nb}}(r_i j) = 4\epsilon_{ij}\left[\left(\frac{\sigma_{ij}}{r_{ij}}\right)^{12} - \left(\frac{\sigma_{ij}}{r_{ij}}\right)^{6}\right] + \frac{q_i q_j}{4\pi\varepsilon_0 r_{ij}}, \tag{S1}$$

where i and j denote non-bonded atoms, q_i and q_j are their respective partial charges, r_{ij} is the separation distance, σ_{ij} is the Lennard-Jones diameter, and ϵ_{ij} is the Lennard-Jones well depth. Heteroatomic interactions are computed with the Lorentz-Berthelot mixing rules,

$$\sigma_{ij} = 0.5(\sigma_{ii} + \sigma_{jj}) \quad \text{and} \quad \epsilon_{ij} = \sqrt{\epsilon_i \epsilon_j}. \tag{S2}$$

Coulombic interactions between atoms separated by three bonds (1-4 interactions) are additionally computed, but the strength of the interaction is reduced by a factor of 0.5, according to the convention of the TraPPE-UA force field.[2,3] The parameters used in the MD simulations for these interactions are provided in Table S1.

Table S1: Non-bonded potential parameters.

atom	m (amu)	σ_{ii} (Å)	ϵ_{ii} ($\frac{\mathrm{kcal}}{\mathrm{mol}}$)	q (e)
ch2	14.02694	3.950	0.091411	0.00
ch3	15.03491	3.750	0.194746	0.00
ce1	13.01897	4.330	0.019872	0.25
ce2	14.02694	3.950	0.091411	0.25
ce3	15.03491	3.750	0.194746	0.25
cm2	14.02694	3.950	0.091411	0.50
oet	15.99940	2.800	0.109296	−0.50
Li^+	6.94100	1.400	0.400000	1.00

1.2 Bonding Potential Parameters

United atoms separated by a single bond interact via a harmonic bonding potential

$$u_{\mathrm{bond}}(r_{ij}) = k_{\mathrm{bond}}(r_{ij} - r_{ij}^{(0)})^2, \tag{S3}$$

where k_{bond} is the bonding force constant, r_{ij} is the separation distance between atom i and j, and $r_{ij}^{(0)}$ is the corresponding equilibrium bonding distance. The parameters used in the MD simulations for this type of interaction are provided in Table S2.

Table S2: Bonding potential parameters for polymer atoms.

bond	k_{bond} ($\frac{\text{kcal}}{\text{mol}\cdot\text{Å}^2}$)	$r_{ij}^{(0)}$ (Å)	bond	k_{bond} ($\frac{\text{kcal}}{\text{mol}\cdot\text{Å}^2}$)	$r_{ij}^{(0)}$ (Å)
ce1 - ch3	225.0	1.540	ce1 - ce2	225.0	1.540
ce2 - ch2	225.0	1.540	ce2 - ch3	225.0	1.540
ce2 - ce2	225.0	1.540	ch2 - ch2	225.0	1.540
ch2 - ch3	225.0	1.540	ce1 - oet	360.0	1.410
ce2 - oet	360.0	1.410	cm2 - oet	360.0	1.410
ce3 - oet	360.0	1.410			

1.3 Bending Potential Parameters

United atoms separated by two bonds interact via a harmonic bending potential

$$u_{\text{bend}}(\theta_{ijk}) = k_{\text{bend}}(\theta_{ijk} - \theta_{ijk}^{(0)})^2, \tag{S4}$$

where k_{bend} is the bending force constant, θ_{ijk} is the angle between atom i, j, and k, and $\theta_{ijk}^{(0)}$ is the corresponding equilibrium angle. The parameters used in the MD simulations for this type of interaction are provided in Table S3.

Table S3: Bending potential parameters for polymer atoms.

bend	k_{bend} ($\frac{\text{kcal}}{\text{mol}\cdot\text{rad}^2}$)	$\theta_{ijk}^{(0)}$ (degrees)	bend	k_{bend} ($\frac{\text{kcal}}{\text{mol}\cdot\text{rad}^2}$)	$\theta_{ijk}^{(0)}$ (degrees)
ch2 - ce2 - oet	49.9782	112.0	ch3 - ce1 - oet	49.9782	112.0
ch3 - ce2 - oet	49.9782	112.0	ce1 - ce2 - oet	49.9782	112.0
ce2 - ce1 - oet	49.9782	112.0	ce2 - ce2 - oet	49.9782	112.0
oet - ce2 - oet	49.9782	112.0	ce2 - oet - ce1	60.0136	112.0
ce2 - oet - ce2	60.0136	112.0	cm2 - oet - cm2	60.0136	112.0
ce2 - oet - ce3	60.0136	112.0	ch3 - ce1 - ce2	62.1001	112.0
ch3 - ch2 - ce2	62.1001	112.0	ce2 - ch2 - ce2	62.1001	114.0
ce2 - ce1 - ce2	62.1001	112.0	[a]oet - cm2 - oet	60.0136	112.0

[a]No explicit parameters are given for this bending type in the TraPPE-UA force field. These values are assumed from a similar bending potential.

1.4 Torsional Potential Parameters

United atoms separated by three bonds interact via potential given by a cosine series

$$u_{\text{tors}}(\phi_{ijkl}) = c_1 \left[1 + \cos\left(\phi_{ijkl}\right)\right] + c_2 \left[1 - \cos\left(2\phi_{ijkl}\right)\right] + c_3 \left[1 + \cos\left(3\phi_{ijkl}\right)\right], \qquad \text{(S5)}$$

where c_1, c_2, and c_3 are constant coefficients, ϕ_{ijkl} is the dihedral angle defined by atoms i, j, k, and l. The parameters used in the MD simulations for this type of interaction are provided in Table S4.

Table S4: Torsional potential parameters for polymer atoms.

torsion	c_1 ($\frac{\text{kcal}}{\text{mol}}$)	c_2 ($\frac{\text{kcal}}{\text{mol}}$)	c_3 ($\frac{\text{kcal}}{\text{mol}}$)	torsion	c_1 ($\frac{\text{kcal}}{\text{mol}}$)	c_2 ($\frac{\text{kcal}}{\text{mol}}$)	c_3 ($\frac{\text{kcal}}{\text{mol}}$)
ch2 - ce2 - oet - ce2	2.882840	−0.650809	2.218510	ch2 - ce2 - oet - ce3	2.882840	−0.650809	2.218510
ch2 - ce2 - oet - ce1	2.882840	−0.650809	2.218510	ch3 - ce2 - oet - ce1	2.882840	−0.650809	2.218510
ch3 - ce2 - oet - ce2	2.882840	−0.650809	2.218510	ch3 - ce1 - oet - ce2	2.882840	−0.650809	2.218510
ce1 - ce2 - oet - ce2	2.882840	−0.650809	2.218510	ce1 - ce2 - oet - ce1	2.882840	−0.650809	2.218510
ce1 - ce2 - oet - ce3	2.882840	−0.650809	2.218510	ce2 - ce2 - oet - ce3	2.882840	−0.650809	2.218510
ce2 - ce1 - oet - ce2	2.882840	−0.650809	2.218510	ce2 - ce2 - oet - ce2	2.882840	−0.650809	2.218510
ce2 - ce2 - oet - ce1	2.882840	−0.650809	2.218510	[a]cm2 - oet - cm2 - oet	2.882840	−0.650809	2.218510
oet - ce1 - ce2 - oet	0.000000	−1.000040	4.000127	oet - ce2 - ce2 - oet	0.000000	−1.000040	4.000127
ch3 - ce1 - ce2 - oet	0.701960	−0.211995	3.060027	ch3 - ch2 - ce2 - oet	0.701960	−0.211995	3.060027
ce2 - ch2 - ce2 - oet	0.701960	−0.211995	3.060027	ce2 - ce1 - ce2 - oet	0.701960	−0.211995	3.060027

[a]No explicit parameters were found for this torsion type in the TraPPE-UA force field. This values are thus approximate and assumed from a similar bending potential.

2 Calculation of Site-refresh Rates

As described in Section 4.2 of the main text, a continuous indicator function $h_i(t) \in (0, 1]$ is defined to facilitate the calculation of the polymer-specific site-refresh rate, ν. In particular, $h_i(t)$ reports on the extent to which a given site i that is identified at time t_i spatially overlaps with any other site after time $t_i \geq t_0$, such that

$$h_i(t) = \max_{\{j\}}[s_{ij}(t_i, t)], \tag{S6}$$

where j ranges over all sites that are identified at t and $s_{ij}(t)$ is a metric for the overlap between site i and site j. This overlap is computed using the Bhattacharyya coefficient [5]

$$s_{ij}(t) = \int_{-\infty}^{\infty} d\mathbf{r} \sqrt{P_i(\mathbf{r}) P_j(\mathbf{r}, t)} \in (0, 1], \tag{S7}$$

where $P_j(\mathbf{r}, t)$ is a Gaussian function that assigns spatial density to site j,

$$P_j(\mathbf{r}, t) = \frac{1}{(2\pi\sigma^2)^{3/2}} \exp\left[-\frac{(\mathbf{r} - \mathbf{r}_j(t))^2}{2\sigma^2}\right]. \tag{S8}$$

Here, $\mathbf{r}_j(t)$ is the Cartesian position of the jth site, and we choose $\sigma = (8 \ln 2)^{-1/2} \sigma_{\mathrm{Li}}$ such that the $s_{ij}(t) = 0.5$ if the coordinates of the sites are separated by a distance σ_{Li}. Although we have employed this particular protocol, we note that there are many possible and reasonable choices for defining both binary and continuous indicator functions for this purpose.

Using eq. (9) of the main text, we find that the data is fit well by a stretched exponential function of the form

$$\mathrm{SACF}(t) = e^{-(t/\alpha)^{\beta}}, \tag{S9}$$

where α and β are independent fitting parameters. Figure S2 shows the data for $\mathrm{SACF}(t)$ for each polymer and the corresponding stretched exponential fit. Using eq. (S9) above with

eq. (10) of the main text yields an expression for the site lifetime

$$\tau_{\text{site}} = \frac{\alpha}{\beta}\Gamma(\beta^{-1}), \tag{S10}$$

where $\Gamma(\cdot)$ denotes the gamma function.

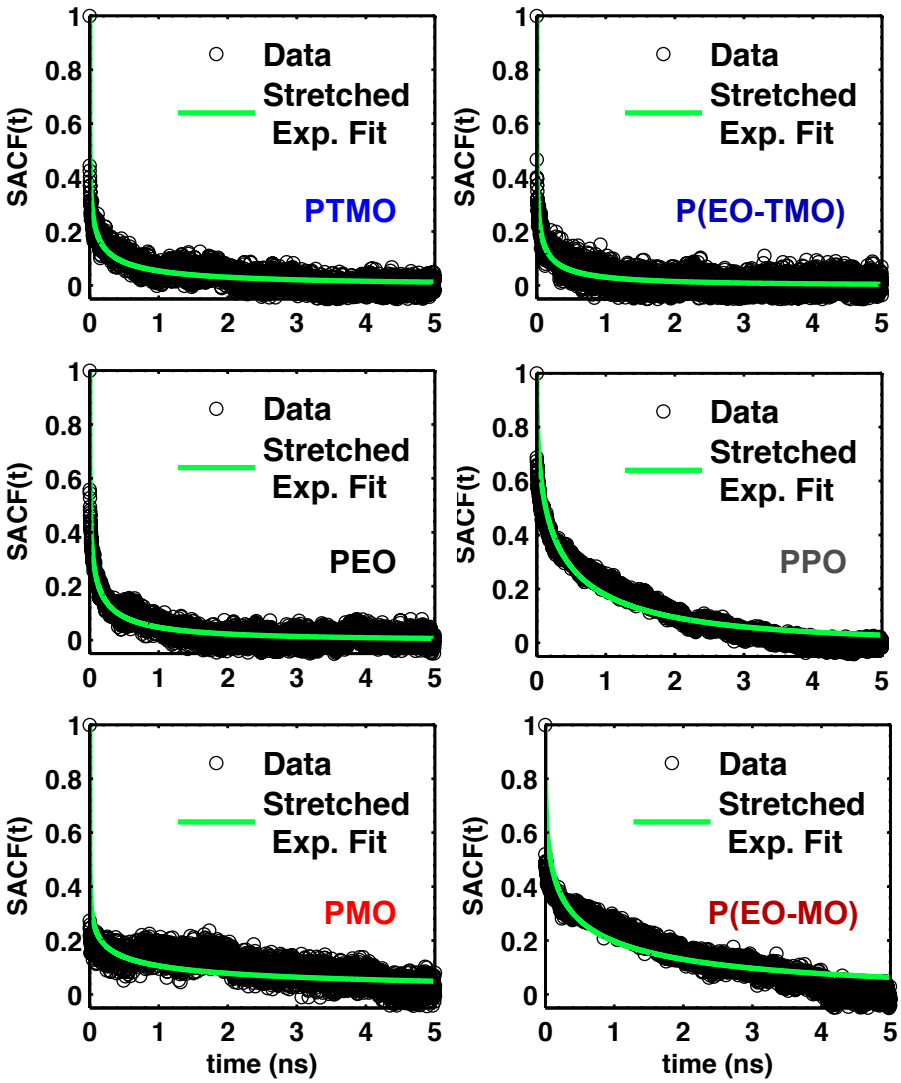

Figure S2: Site autocorrelation function data and corresponding stretched exponential fit for each polymer studied.

3 Convergence of the Polymer Bulk Modulus

Figure S3 shows the running average of the bulk modulus, as obtained from volume fluctuations in the NPT ensemble. The figure shows that the bulk modulus for all polymers is fairly well-converged after only a few nanoseconds of simulation. Additionally, the relative values of the bulk moduli among the various polymers seem converged after just 1 ns of averaging.

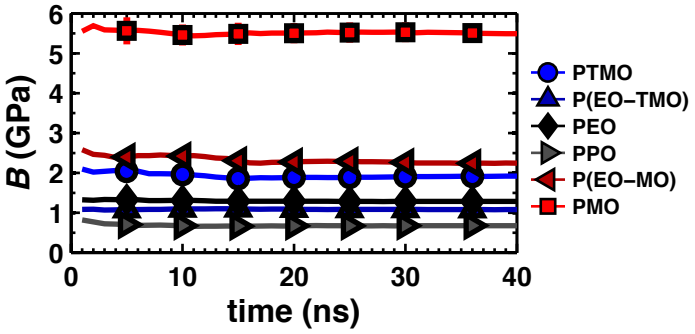

Figure S3: Running average of the bulk modulus estimate as a function of time for each polymer. Error bars are the standard error of the mean obtained from four independent trajectories.

4 Iterative Boltzmann Inversion for the Lithium-site RDFs

To generate configurations of sites that satisfy the pair radial distribution functions (RDFs) obtained from MD snapshots, an iterative Boltzmann (IBI) procedure is used.[?] Although the IBI procedure works well for reproducing the site-site radial distribution function (Figure 9 of the main text), Figure S4 illustrates that the procedure was less robust in application to the lithium-site RDF.. The difficulty in converging the lithium-site RDFs is partially due to the fact that reference distributions are not smooth due to worse sampling statistics; moreover, previous work has pointed out that there is no guarantee that a pair potential exists to reproduce the lithium-site RDF from the site density.[6]

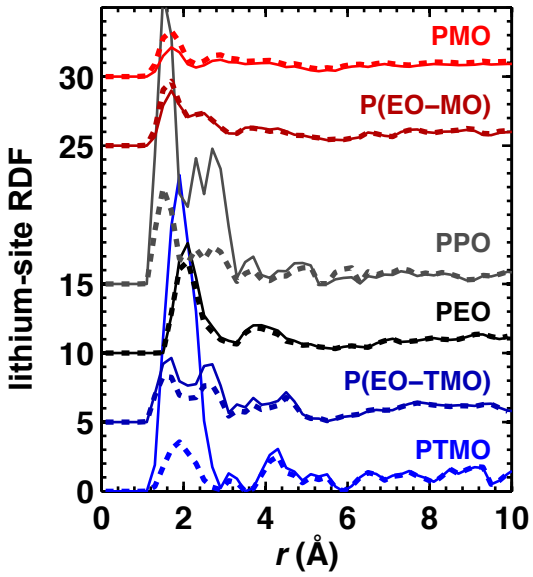

Figure S4: Lithium-site radial distribution functions (RDF) obtained from MD (solid lines) and from IBI (dashed lines). For clarity, the data for P(EO-TMO), PEO, PPO, P(EO-MO), and PMO are shifted vertically by 5, 10, 15, 25, and 30 units, respectively.

5 Comparison of Lithium-ion Mean-square Displacements on Logarithmic Axes

To indicate the power-law scaling between the lithium-ion mean-square displacement and time, Figure S5 shows the same data from Figure 12 of the main text with logarithmic scaling for both axes. Figure S5A illustrates the difficulty in obtaining diffusion coefficients from brute-force, atomistic MD since very few of the polymers, if any, have reached the fully diffusive regime after 150 ns. In Figure S5B, the KMC simulations of some of the polymers also exhibit a transition from sub-diffusive to diffusive behavior. However, given that the KMC simulations do not include co-diffusion of the lithium cation with the coordinating polymer, this sub-diffusive behavior arises due to hopping within a localized cluster of sites and not due to local co-diffusion with the chain segments.

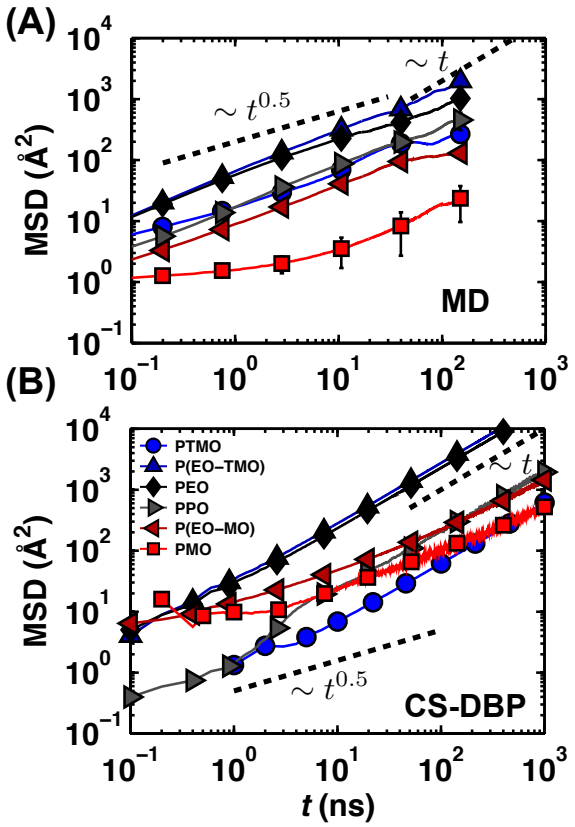

Figure S5: Mean square-displacement of lithium cation obtained from (A) MD simulation and (B) the CS-DBP model with logarithmic scaling on the x- and y-axis. The dashed lines are guides to eye for identifying power law scaling.

References

(1) Vanommeslaeghe, K.; Hatcher, E.; Acharya, C.; Kundu, S.; Zhong, S.; Shim, J.; Darian, E.; Guvench, O.; Lopes, P.; Vorobyov, I.; Mackerell, A. D. *Journal of Computational Chemistry* **2010**, *31*, 671–690.

(2) Martin, M. G.; Siepmann, J. I. *The Journal of Physical Chemistry B* **1999**, *103*, 4508–4517.

(3) Stubbs, J. M.; Potoff, J. J.; Siepmann, J. I. *The Journal of Physical Chemistry B* **2004**, *108*, 17596–17605.

(4) Wu, H.; Wick, C. D. *Macromolecules* **2010**, *43*, 3502–3510.

(5) Bhattacharyya, A. *Bull. Calcutta Math. Soc.* **1943**, *35*, 99–109.

(6) Henderson, R. *Phys. Lett. A* **1974**, *49*, 197 – 198.